Formation of Polysaccharide Gel Layers in the Presence of Ca^{2+} and K^{+} Ions: Measurements and Mechanisms

Alexis J. de Kerchove and Menachem Elimelech*

Department of Chemical Engineering, Environmental Engineering Program, Yale University, P.O. Box 208286, New Haven, Connecticut 06520-8286

Received July 11, 2006; Revised Manuscript Received October 1, 2006

Understanding the adsorption properties of polysaccharides in terms of substrate affinity, kinetics, and layer structure is of paramount importance in numerous industrial and natural systems. The structural growth of the layers of two model polysaccharides—sodium alginate and polygalacturonic acid (PGA)—was characterized by quartz crystal microbalance with dissipation and atomic force microscopy. Monitoring the variations in frequency and dissipation energy provides insights into both the average adsorbed mass and the viscoelastic properties of the adsorbed layer of polyelectrolytes along with the associated ions and water molecules. Both polysaccharides had similar adsorption patterns with increasing ionic strengths and showed significant complexation of calcium ions. In the presence of calcium, the alginate gel layer exhibited significant swelling with an increasing concentration of monovalent salt that the PGA gel layer did not manifest. Basing our discussion on the "egg-box model", we interpreted these different swelling behaviors as resulting from differences in the complexation modes of the two polysaccharides. The dimerization of the polymers by cross-linking and the weaker dimer−dimer associations play major roles in the sensitivity of the polysaccharide gel matrix to high salt concentration environments.

1. Introduction

Polygalacturonic acids (PGAs) and alginates are natural ionic polysaccharides that have extensive use within the textile,[1] food,[2] and biomedical[3] industries. These applications are based on polyelectrolyte multilayer coating or microencapsulation techniques.[4−7] Such techniques rely on the high electrostatic charges of polysaccharides and on their ability to form gel-like structures in the presence of divalent cations. PGAs, also commonly called polypectates, have a linear backbone of (1→4)-linked α-D-galacturonic acid and do not display the various heterogeneities typical of pectins, such as methanol esterification, α-L-rhamnopyranosyl residues, and side chains of neutral sugars.[8,9] Alginates also adopt a linear backbone composed of pattern blocks of homopolymeric regions of (1→4)-linked β-D-mannuronic and (1→4)-linked α-L-guluronic acid β.[10,11]

The gelation of these polyelectrolytes results from the strong interactions between divalent cations and blocks of either galacturonic or guluronic acid residues for PGA[8] and alginate,[12] respectively. Due to their backbone heterogeneity, alginates have a specific gelation efficiency depending on the mannuronic/guluronic acid content ratio.[13,14] PGAs form strong gels due to the high specificity of galacturonic acids to calcium binding and the homogeneity of their backbones. For both of these polysaccharides, the gel structure results from the formation of junction zones by the association of the polymer chains in the presence of calcium ions. The "egg-box model" is used to describe the junction zones of alginate and pectate gels.[15] This model suggests that helical chains strongly associate by the specific sequestration and binding of calcium ions. Subsequent aggregation of dimers also contributes to the final structure of the gel.

The major differences in the backbone structures of these two polysaccharides affect their efficiency to form gels in the presence of calcium, which, subsequently, determines the physicochemical properties of the gel.[16] These properties, such as viscoelasticity, highly depend on the ionic composition of the surrounding solution. However, the response of the gel layer to variation in ionic strength is likely to vary for these polysaccharides in accordance with their ability to form calcium bonds. These specific bindings are assumed to be more stable with respect to ionic strength changes than nonspecific electrostatic interactions. Conventional experimental techniques used to study polysaccharide gel properties are unsuitable for studying the continuous evolution of these properties as a function of solution chemistry.[17−20] A direct correlation between the evolution of the layer structural properties and the specificities of the molecular backbone to form gel complexes has never been shown. Such a correlation could confirm the speculative nature of the proposed model of gelation in the presence of divalent cations.

Recently, we have used a quartz crystal microbalance with dissipation (QCM-D) and atomic force microscopy (AFM) to study the growth of a polysaccharide layer in situ in real time as a function of the solution chemistry.[21] The basic principles of these two instruments have been extensively described in the literature.[22−26] The combination of the QCM-D and AFM results has been shown to complement studies of polymer layers adsorbed at solid interfaces.[27−30] Adsorbed layer structural information obtained by the QCM-D, such as the layer thickness and rigidity, can be associated with the interaction forces between the adsorbed polysaccharides measured by AFM.

The salt concentration of the bulk solution also has an important impact on the gelation of polysaccharides. The displacement of the ion-exchange equilibrium at high ionic strength was shown to be occurring within the complexed gel matrix as a result of the replacement of the divalent calcium ions with monovalent cations.[31−33] Such an ion-exchange process greatly influences the structure and integrity of the gel

* Author to whom correspondence should be addressed. Phone: (203) 432-2789. Fax: (203) 432-2881. E-mail: menachem.elimelech@yale.edu.

10.1021/bm060670i CCC: $37.00
Published on Web 12/06/2006

matrix. Our previous study showed that the ion-exchange process induced the swelling and disintegration of alginate gel layers.[21]

Our main goal in this paper is to study the impact of increasing ionic strength on the structure of the calcium-induced gel matrix of two commonly used polysaccharides. We compared the viscoelastic properties of the gel layer to the polysaccharide−polysaccharide interaction forces as a function of the bulk solution salt concentration. Understanding the evolution of the structural properties and cohesive interaction forces for both alginate and PGA gel layers helps us to explore the role of the backbone structure in the ion-exchange process. Results could also demonstrate the relevance of the egg-box model suggested for both galacturonate and guluronate residues.

2. Materials and Methods

2.1. Polysaccharides and Solution Chemistry. Sodium alginate, derived from the alga *Macrocistys pyrifera*, and PGA, with molecular weight ranges of 12−80 and 25−50 kDa, respectively, were obtained from Sigma (St Louis, MO). The percentages of mannuronic and guluronic blocks in the sodium alginate are 39% and 61%, respectively. Sodium alginate was dissolved in deionized water (Barnstead) at ambient pH (pH 5.5−5.7), and the stock solution (2 g L^{-1}) was stored at 4 °C. PGA was gradually dissolved in deionized water by maintaining the pH at 6.5 with KOH to obtain a final concentration of 2 g L^{-1}. The final solution was filtered through a 0.22 μm filter (Millipore Corp., Billerica, MA) and stored at 4 °C. Both polysaccharides were used at a final concentration of 0.1 g L^{-1}, which was achieved by diluting the stock solution in the electrolyte solution of interest at ambient pH immediately prior to the adsorption experiment. Both polysaccharides have pK_a values between 3.3 and 3.6 and are thus negatively charged at ambient pH. The carboxylic acidity of both polysaccharides was measured by potentiometric titration (794 Basic Titrino, Metrohm, Herisau, Switzerland).

Electrolyte solutions were prepared with deionized water and reagent grade salts (Fisher) and stored at 4 °C. Polysaccharide adsorption was studied over a range of ionic strengths (3−300 mM) by varying monovalent electrolyte (KCl) concentrations. The effect of calcium was studied by adding to the solution the maximum concentration of calcium that would not induce the formation of visually detectable aggregates in solution. To achieve this condition, $CaCl_2$ was added at a concentration of 1 mM for alginate and 0.1 mM for PGA.

2.2. QCM-D. The quartz crystal microbalance with dissipation (QCM-D 300, Q-Sense AB, Gothenburg, Sweden) is operated at its fundamental frequency of 5 MHz. Data from the third, fifth, and seventh overtones (working at the resonance frequencies of 15, 25, and 35 MHz) were used to calculate the viscoelastic properties of the film. The QCM-D was used in continuous flow-through mode. A flow of 0.1 mL min^{-1} was induced with a syringe pump (KD Scientific Inc., New Hope, PA) in suction mode at the exit of the QCM-D chamber. Calculations of the film thickness, elastic shear modulus, and shear viscosity are based on the Voigt model presented by Voinova et al.[34,35] by assuming a film density of 1030 kg m^{-3}. The thickness and density of the film were assumed to be uniform. Fitting of the results was done using the program Q-Tools provided by Q-Sense AB.

2.3. AFM. A NanoScope IIIa multimode atomic force microscope (Digital Instruments, Santa Barbara, CA) was used to measure adhesion forces between polysaccharides adsorbed at the solid interface. Because carboxylic groups are the predominant functional groups of our polysaccharides, a carboxylated modified latex (CML) particle (Interfacial Dynamic Corp., Portland, OR) was used as a surrogate for alginate and PGA. The CML particle (4 μm in diameter) was covered with a porous and highly charged polyelectrolyte layer that is rich in carboxylated groups and has a titrated surface charge of 139.5 μC cm^{-2}. A colloid probe was made by attaching the particle to a tipless Si_3N_4 cantilever, having a spring constant of 0.06 N m^{-1} (Veeco Metrology Group, Santa Barbara, CA). A drop of CML colloidal suspension was first spread on a freshly cleaved mica surface and dried with Ar gas. With a laboratory-fabricated micromanipulator, a small amount of glue (Norland Optical Adhesive, Norland Products, Inc., Cranbury, NJ) was spread on the free end of the tipless Si_3N_4 probe. A single CML particle was then attached to the cantilever end, allowing only a small surface area of the particle to come in contact with the glue. The glue was cured for 15 min under UV irradiation. The strength of the colloid probe was tested by applying forces to the attached particle from different angles using another unmodified cantilever. A new colloid probe was used for each experiment. The probes were carefully examined before and after their use to ensure their integrity.

Force measurements were conducted in a fluid cell with a closed input and output. The solution conditions tested were similar to those used in the QCM-D adsorption experiments. The different steps involved in the polysaccharide adsorption were conducted under flow conditions. A flow of 0.2 mL min^{-1} was induced with a syringe pump (model 200 syringe pump, KD Scientific Inc., New Hope, PA) in suction mode at the exit of the liquid chamber. An additional resting period of 15 min was allowed at the end of the conditioning and rinse periods (described in the following section) before force measurements were conducted to stabilize the system and optimize the AFM signal. Because of surface heterogeneities, force measurements were conducted at five different locations, with a minimum of ten replicates at each location. Adhesion forces were obtained by operating the atomic force microscope in contact mode.

The raw data, consisting of cantilever deflection versus cantilever displacement, were first processed to remove optical interference. The resulting curves were then converted to force normalized by the colloid probe radius (F/R) versus surface-to-surface separation curves, using the method reported by Ducker et al.[36] The maximum adhesion force and the maximum pull-off distance were extracted from each coherent force curve. Averages of these parameters and standard deviations were calculated within a 90% confidence interval.

2.4. Polysaccharide Adsorption Protocol. Polysaccharide adsorption and layer growth were induced under flow conditions. The ionic strength was increased incrementally during the course of the experiment. Details on the protocol and the sequence of the adsorption experiment can be found in our recent study.[21]

AT-cut quartz crystals with SiO_2 coating (Q-sense AB, Gothenburg, Sweden) were used for the adsorption experiments in the QCM-D. For the AFM studies, the substrate used was a 10 mm × 10 mm × 1 mm quartz microscope slide (Electron Microscopy Sciences, Hatfield, PA). Surfaces were cleaned for a minimum of 4 h in a 2% Hellmanex II solution (Hellma GmbH & Co. KG, Müllheim, Germany), maintained at 50 °C, rinsed thoroughly with deionized water, and oxidized for 15 min in an UV/O_3 chamber. Favorable conditions for initial alginate adsorption onto the silica surface were established by adsorbing a conditioning layer of poly-L-lysine (PLL) onto the silica or quartz surface. Poly-L-lysine hydrobromide (Sigma) was used. Cationic PLLs have a molecular weight ranging from 70 to 150 kDa. PLL was dissolved in HEPES buffer (pH 7.4) made from 10 mM *N*-(2-hydroxyethyl) piperazine-*N*′-2-ethanesulfonic acid (Sigma), 100 mM KCl, and deionized water, and stored at 4 °C. The final concentration of the stock PLL solution was 0.4 g L^{-1}. QCM-D results showed that an exposure of the SiO_2 substrate surface to the PLL stock solution for 15 min was enough to create a homogeneous layer.

The conditioning PLL film was rinsed three times, each for 15 min, with the electrolyte solution used for the following (first) polysaccharide adsorption experiment. An initial layer of polysaccharide was adsorbed onto the PLL layer for 15 min, responding to attractive PLL−polysaccharide electrostatic interactions. Consecutive sublayers of polysaccharide were adsorbed onto the initial layer at increased ionic strengths to study the impact of polysaccharide−polysaccharide interactions on layer growth and structure. The formation of each of these sublayers involves, first, the conditioning of the existing layer for 15

min with the new electrolyte solution to induce the ionic strength shift. The conditioning is followed by polysaccharide adsorption for a period of 15−90 min, until the measured shifts in frequency and dissipation given by the QCM-D become small enough to be disregarded. The final step of the sublayer formation consists of rinsing the layer for 15 min with the same electrolyte solution that was used for conditioning.

2.5. Analysis of Polysaccharide Layer Properties. Properties of the adsorbed layer were extracted at the end of the conditioning and rinse periods. This involved either the force measurement being taken by AFM or the averaging of 5 min of the fitted response given by the QCM-D at the end of each of these periods. The analysis of the data was based on the calculation of changes in the layer properties as a function of ionic strength. The impact of ionic strength variations on the measured layer properties, called the "electrolyte effect", was analyzed by comparing the differences in layer properties measured at the end of the conditioning period at a specific ionic strength to those measured during the rinse period at the preceding lower ionic strength. The change in layer properties caused by the adsorption of polysaccharides at a specific ionic strength was also analyzed. The "incremental adsorption" is the difference in property values between the rinse and the conditioning period of the same sublayer at a specific ionic strength.

3. Results and Discussion

The growth and evolution of the viscoelastic properties of the polysaccharide layer are studied by combining results obtained from the QCM-D and AFM investigations. The impacts of calcium and variation in ionic strength on polysaccharide gelation and the resulting properties of the adsorbed layer are extracted from the analysis of different sets of results. The QCM-D provides information on variations in the thickness as well as the rigidity of the layer as it grows in response to polysaccharide adsorption and swelling. AFM measures the intermolecular adhesion forces that characterize the polysaccharide−polysaccharide interactions in the adsorbed layer.

3.1. Variation of the Polysaccharide Layer Thickness. Film thickness is measured by QCM-D and is shown to greatly vary as a function of the salt composition as seen in Figure 1. In the absence of calcium, polysaccharide adsorption is highly favored by increasing the ionic strength (Figure 1a). At lower ionic strengths, alginate adsorption is observed to be more favorable than PGA adsorption. Incremental thickness resulting from the incremental adsorption begins to increase significantly at ionic strengths of 10 and 100 mM KCl for alginate and PGA, respectively (Figure 1b), which suggests that larger electrostatic repulsion forces may control the adsorption of PGAs. To verify this hypothesis, we performed a potentiometric titration of both polysaccharides, which showed that the carboxylic acidity at ambient pH (pH 5.5−5.7) is 10.5 mequiv/g carbon for alginates and 11.5 mequiv/g carbon for PGA. This higher charge density for PGAs may explain the electrostatic stabilization of these polysaccharides observed over a wide section of the studied ionic strength range. The absence of proportionality between changes in thickness and increases in ionic strength and the differences in incremental thickness variation between polysaccharides reveal the complexity of interactions between the adsorbing material (i.e., polysaccharides, water, and salts). A detailed discussion of the forces controlling these interactions in the absence of calcium is available in our recent study on alginate layer formation in a batch system.[21]

The presence of calcium in solution induces significant adsorption of both polysaccharides at the quartz surface (Figure 1c); however, the absorbed layer was observed to be insensitive to increases in ionic strength after initial adsorption. The largest incremental adsorption of both polysaccharides occurs on the

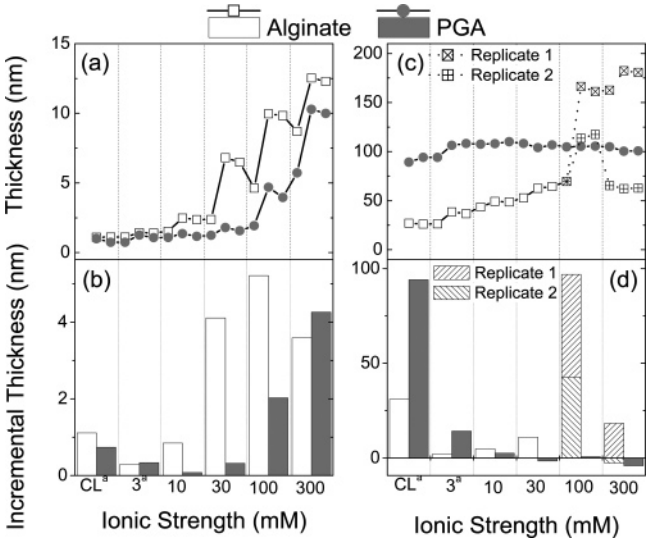

Figure 1. Evolution of the thickness of the adsorbed polysaccharide layers obtained by QCM-D as a function of ionic strength: (a) in monovalent salt and (c) in the presence of calcium. For the adsorption of alginate on the PLL (CL), the first two data points are for alginate adsorption and layer rinsing with the background electrolyte; the conditioning of the PLL layer is not shown. The thickness is offset at zero after the rinse of the PLL layer. For each subsequent condition, measurements shown correspond to the conditioning of the existing layer, the adsorption of alginate, and the rinse of the layer with the background solution. Incremental variations of the thickness resulting from the polysaccharide adsorption are also shown for (b) adsorption with monovalent salt and (d) adsorption in the presence of calcium. The incremental variations are obtained as defined in the text. The optimal fittings for the thickness are obtained considering the third, fifth, and seventh harmonics using the Voigt-based model for a single-layer system.

PLL conditioning layer (Figure 1d) in which initial adsorption was observed to be at least 40 times thicker than that in scenarios run in the absence of calcium. PGAs consistently adsorbed in a layer twice as thick as the alginate layer on PLL; however, subsequent incremental adsorption involving PGA−PGA or alginate−alginate interactions was typically insignificant. An exception is alginate adsorption at high ionic strength (i.e., >100 mM) in which alginate incremental adsorption induced a major increase in the layer thickness. Figures 1c and 1d show the evolution of the alginate layer thickness for two replicate experiments. For both replicates, the incremental thickness obtained at 100 mM ionic strength is significant, suggesting that alginate adsorption could be important at that ionic strength in addition to the swelling of the layer.[37]

The electrolyte effect is associated with the change of electrolyte between the conditioning period at a specific ionic strength and the rinse period at the preceding ionic strength. In the absence of calcium (Figure 2a), electrolyte transitions have no significant impact on the thickness of the layers (i.e., always less than 2 nm). In the presence of calcium (Figure 2b), ionic strength transitions have insignificant effects on the PGA layer thickness; however, the alginate layer shows a constant swelling in response to transitions in salt concentration. Such swelling is maintained over the entire ionic strength range until 300 mM KCl (Figures 1b and 2b). Replicate experiments show that two different behaviors of the layer can be observed. During the transition from 100 to 300 mM KCl, the adsorbed layer either maintains its structure or is subject to a major decrease in layer thickness. Such variability in the responses of the adsorbed layer to changes in salt concentration at high ionic strength is an indication of the fragility of the alginate layer. It is likely that

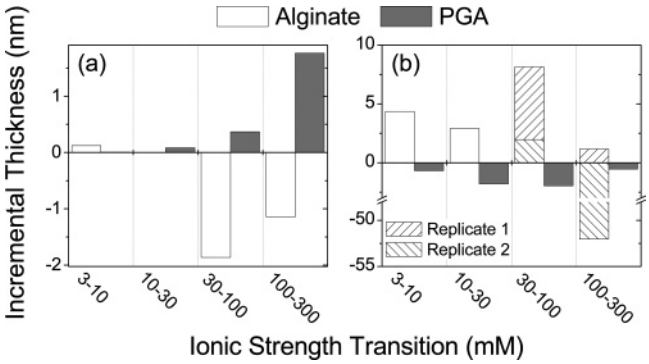

Figure 2. Incremental variations of the thickness resulting from ionic strength transitions (so-called "electrolyte effect") obtained by QCM-D (a) in monovalent salt only and (b) in the presence of calcium. The incremental variations are obtained as defined in the text. The optimal fittings for the thickness are obtained considering the third, fifth, and seventh harmonics using the Voigt-based model for a single-layer system.

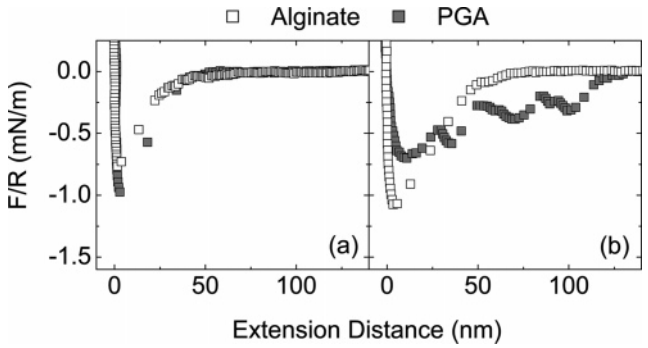

Figure 3. Representative adhesion force profiles between the AFM colloidal probe and the quartz substrate coated with either alginate or PGA film at a total ionic strength of 10 mM (adjusted with KCl). Adhesion force profiles measured (a) in the absence and (b) in the presence of calcium are shown for both polysaccharides.

in the best circumstances, the change in ionic strength induces a minor swelling of the adsorbed layer. However, a significant increase in layer thickness at 100 mM could have weakened the layer, and subsequent changes in ionic strength (100−300 mM) could result in further swelling of the layer and degradation of the film by alginate desorption.

These major differences observed between alginates and PGAs show varying degrees of stability of the adsorbed layer in response to cumulative polymer adsorption and ionic strength changes. It is shown that the presence of calcium plays a major role not only in the adsorption of alginate to PLL under favorable interactions but also in the cohesion of the layer structure as surrounding salt conditions change.

3.2. Variation of Intermolecular Interaction Forces. Normalized adhesion forces (F/R), which characterize interactions between the polysaccharide layer and the newly absorbed polysaccharides,[38] are measured prior to polysaccharide adsorption as a function of ionic strength. Representative adhesion force profiles between the polysaccharide layer and the AFM probe are shown in Figure 3. These force profiles, measured at a total ionic strength of 10 mM, illustrate the impact of calcium on the measured force profiles for both polysaccharides. Because of the inherent heterogeneity in the adhesion force measurements, the averages of the adhesion forces along with the corresponding standard errors are shown in Figure 4 for each of the ionic strengths investigated. In monovalent salts (Figure 4a), measured interaction forces for both polysaccharides are consistently of the same order of magnitude (i.e., $F/R = 0-1$ mN m^{-1}) and are shown not to vary significantly with increases in ionic strength. Adhesion forces between polysaccharides and the PLL conditioning layer (data not shown) were always at least an order of magnitude higher ($F/R = -4.5 \pm 0.5$). Lower adhesion forces are observed for alginates at ionic strengths between 10 and 100 mM in comparison to those for PGAs. This difference might be attributed to the PGA's smaller range of molecular weights. Smaller molecules most likely exhibit lower steric hindrance in their interactions with the adsorbed layer, which could result in stronger adhesion forces.

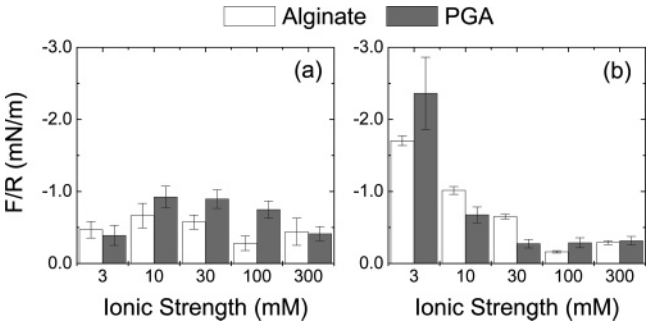

Figure 4. Variation of adhesion forces between the AFM colloidal probe and the existing adsorbed polysaccharide layer as a function of ionic strength (a) in the absence and (b) the presence of calcium. Adhesion forces are determined from the retraction of the AFM colloid probe from the surface prior to the alginate adsorption step at a specific ionic strength. Adhesion forces are normalized by the radius of the colloidal probe (F/R). Error bars represent one standard error.

In the presence of calcium (Figure 4b), both polysaccharides display stronger adhesion forces (i.e., $F/R > 1$ mN m^{-1}) at low ionic strength (3 mM). As the ionic strength increases, forces gradually decrease to a level similar to that observed in the absence of calcium. Differences in the specific ability of each polysaccharide to complex divalent calcium ions are demonstrated when interaction forces are compared to the thickness analyses. Initial strong adhesions can be attributed to gel matrix formation between polysaccharides by sequestration of calcium ions. The higher efficiency of PGAs to complex calcium ions is directly perceived by the formation of a thicker layer involving stronger adhesive interactions.

As monovalent salt concentrations are increased, weakening of adhesion bonds is observed for both polysaccharides. Such a trend could be induced by an increasing competition between monovalent and divalent cations for charged moieties on the polysaccharide backbone. This ion-exchange process is discussed in depth later in the paper.

3.3. Viscoelastic Properties of Polysaccharide Layers. Viscoelastic properties (i.e., elastic shear modulus and the shear viscosity) of the adsorbed layer are obtained by modeling the QCM-D experimental data. This best fitting procedure involves adjusting three parameters on the basis of shifts in frequency, $\Delta f_{(n)}$, and shifts in dissipation, $\Delta D_{(n)}$, measured for three harmonics, n. Since the best fitting values may not necessarily represent the most meaningful values,[27] $\Delta D_{(n)}$ versus $\Delta f_{(n)}$ charts are generated in Figure 5. These plots provide useful qualitative insights into the viscoelasticity variations during the formation of the polysaccharide film. For this figure, the third harmonic (resonance frequency of 15 MHz) was used. Plots generated from the fifth and seventh harmonics showed similar trends (data not shown). Each curve segment characterizes the incremental adsorption of polysaccharides at a specific ionic strength for a time period ranging from 15 to 90 min. The polysaccharide adsorption induces a reduction of the resonance frequency of the quartz and an increase in its dissipation. Similar trends in

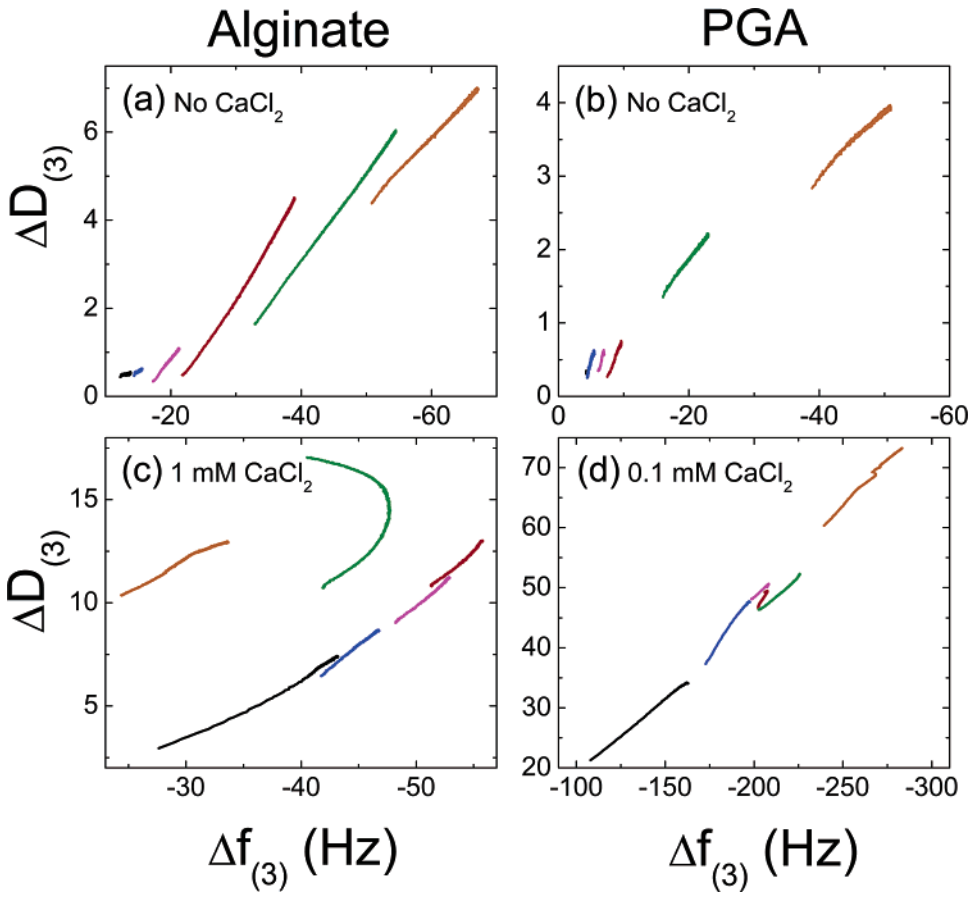

Figure 5. Variations in dissipation as a function of frequency shifts observed in the QCM-D during the polysaccharide adsorption phases. ΔD vs $\Delta f_{(3)}$ plots are shown for alginate adsorption (a) in the absence and (c) in the presence of calcium (only data for replicate 1 are shown) and for PGA adsorption (b) in the absence and (d) in the presence of calcium. Dissipation variations are measured during the conditioning layer stage (corresponding to a polysaccharide/PLL layer) at 3 mM ionic strength (in black) and during the successive alginate adsorptions at ionic strengths of 3 (in blue), 10 (in pink), 30 (in red), 100 (in green), and 300 mM (in orange). Data from the 15 MHz resonance were used.

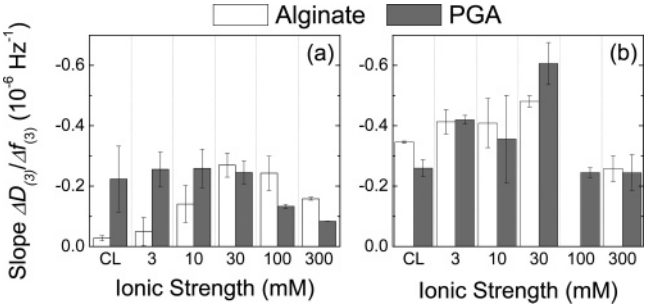

Figure 6. Estimation of the variation in layer rigidity (defined by the ratio $\Delta D_{(3)}/\Delta f_{(3)}$) during the polysaccharide incremental adsorption. Calculated slopes as a function of ionic strength are shown for both polysaccharides (a) in the absence and (b) in the presence of calcium. The slope $\Delta D_{(3)}/\Delta f_{(3)}$ characterizing the alginate layer in the presence of calcium at 100 mM ionic strength could not be calculated due to the nonlinearity of the $\Delta D_{(3)}/\Delta f_{(3)}$ relationship (shown in Figure 5). Error bars represent one standard deviation.

the variation of dissipation with frequency shift are observed at various ionic strengths, and linear dependences are obtained in most cases.

The magnitudes of the slopes of the linear relationships shown in Figure 5 are presented in Figure 6. These $\Delta D_{(3)}/\Delta f_{(3)}$ ratios indicate the variations in the rigidity of the adsorbed layer, with a smaller ratio characterizing a more rigid layer. The rigidity of the layer is assumed to be related to the water trapped in the polysaccharide matrix that provides fluidity to the film. The results in Figure 6 may imply that the gelation of polysaccharides in the presence of calcium results in the formation of a highly fluid layer. This is supported by the high $\Delta D_{(3)}/\Delta f_{(3)}$ ratios obtained for both polysaccharides in the presence of calcium. At 100 mM ionic strength, an abrupt change of the layer structure is suggested based on the decrease in the $\Delta D_{(3)}/\Delta f_{(3)}$ ratio (Figure 6b). This phenomenon is especially notable for the alginate layer. The $\Delta D_{(3)}/\Delta f_{(3)}$ relationship loses its linearity as depicted in Figure 5c in the replicate experiment 1. Replicate experiment 2 also showed a very similar nonlinear behavior (data not shown). The fitting of the viscoelastic parameters previously introduced could help the interpretation of this phenomenon.

The variations of the two viscoelastic parameters fitted with our experimental data—the elastic shear modulus and the shear viscosity—over the entire ionic strength range are shown in Figure 7. These variations are quantitatively represented in Table 1 by a parameter that we denote as the coefficient of variation, C. The coefficients of variation are calculated for the elastic shear modulus and the shear viscosity over each transition in electrolyte concentration or adsorption stage examined during the experiment. The definitions of the coefficients of variation calculated for the electrolyte effect and the incremental adsorption (described in section 2.5) are given by

$$C_{(\text{electrolyte effect})} = \frac{X_{(\text{conditioning period})}(\text{IS}_{(i)})}{X_{(\text{rinse period})}(\text{IS}_{(i-1)})} \quad (1)$$

$$C_{(\text{incremental adsorption})} = \frac{X_{(\text{rinse period})}(\text{IS}_{(i)})}{X_{(\text{conditioning period})}(\text{IS}_{(i)})} \quad (2)$$

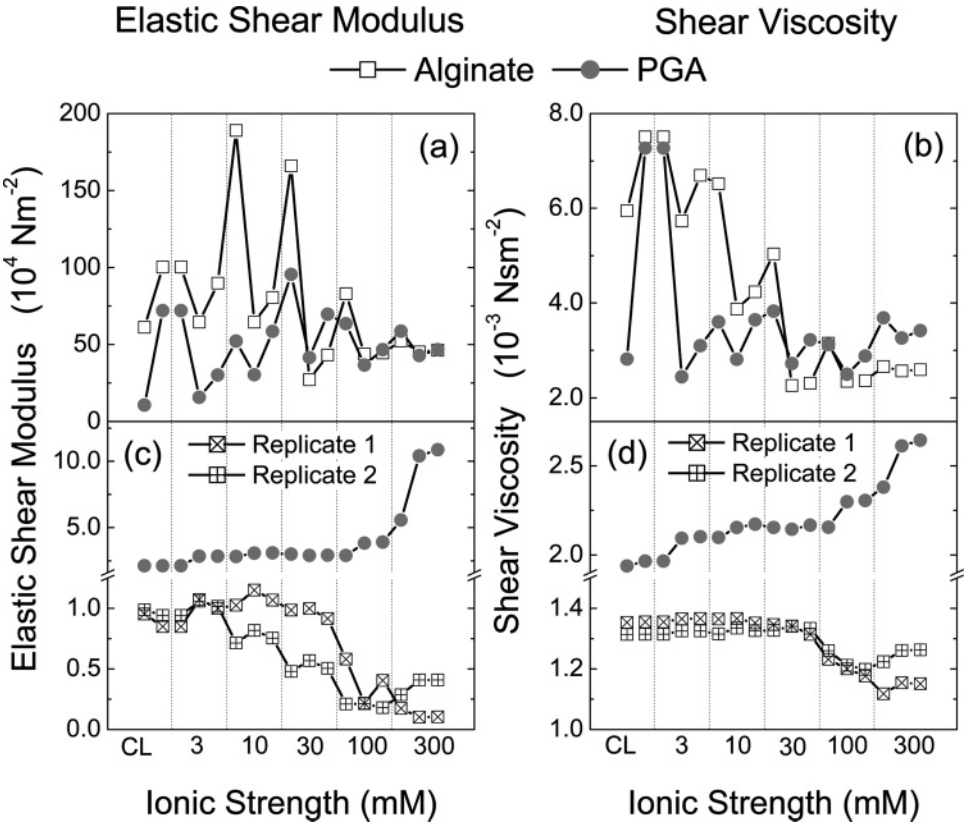

Figure 7. Variations in viscoelastic properties of the adsorbed polysaccharide layer: changes in elastic shear modulus (a) in the absence and (c) in the presence of calcium and changes in shear viscosity (b) in the absence and (d) in the presence of calcium. The optimal fittings for this parameter are obtained considering the third, fifth, and seventh harmonics using the Voigt-based model for a single-layer system.

Table 1. Coefficients of Variation (C) of the Elastic Shear Modulus and Shear Viscosity of the Adsorbed Layer[a]

ionic strength transition (mM)										
	elastic shear modulus					shear viscosity				
	$C_{(\text{electrolyte effect})}$					$C_{(\text{electrolyte effect})}$				
	no $CaCl_2$		$CaCl_2$			no $CaCl_2$		$CaCl_2$		
			alginate					alginate		
	alginate	PGA	R_1	R_2	PGA	alginate	PGA	R_1	R_2	PGA
3−10	2.1	1.7	1.0	0.7	1.0	1.0	1.2	1.0	1.0	1.0
10−30	2.1	1.6	0.9	0.6	1.0	1.2	1.0	1.0	1.0	1.0
30−100	2.4	0.9	0.6	0.5	1.0	1.4	1.0	0.9	0.9	1.0
100−300	1.3	1.3	0.4	1.5	1.4	1.1	1.3	1.0	1.0	1.0
ionic strength (mM)										
	$C_{(\text{incrementa adsorption})}$					$C_{(\text{incremental adsorption})}$				
	no $CaCl_2$		$CaCl_2$			no $CaCl_2$		$CaCl_2$		
			alginate					alginate		
	alginate	PGA	R_1	R_2	PGA	alginate	PGA	R_1	R_2	PGA
3	0.9	0.4	1.2	1.1	1.3	0.9	0.4	1.0	1.0	1.1
10	0.4	1.1	1.0	1.1	1.1	0.6	1.0	1.0	1.0	1.0
30	0.2	0.7	0.9	1.1	1.0	0.5	0.8	1.0	1.0	1.0
100	0.4	0.7	0.7	0.9	1.4	0.7	0.9	1.0	1.0	1.1
300	0.8	0.8	0.5	1.4	2.0	1.0	0.9	1.0	1.0	1.1

[a] C represents a variation in viscoelastic properties resulting from the electrolyte effect and the incremental adsorption at all ionic strengths. Results for both studied replicate experiments (R_1 and R_2) are shown for alginate adsorption in the presence of calcium.

where X is the studied viscoelastic property measured at a specific experimental step and ionic strength and $IS_{(i)}$ and $IS_{(i-1)}$, with i varying from 1 to 5, are the studied ionic strengths (from 3 to 300 mM).

Both fitted parameters show that the viscoelasticity of the polysaccharide layers follows similar trends as those predicted by the $\Delta D_{(3)}/\Delta f_{(3)}$ analysis. In monovalent salts only, both polysaccharides show similarly rigid layers, suggesting poor water content. The viscoelastic parameters are, however, very scattered and reach some absurdly large values in some cases (Figure 7). The amplitude of these variations is perceived in Table 1. Such scattering points out the difficulty in using the Voigt-based model to fit the viscoelastic parameters in the case of a rigid layer.

In the presence of $CaCl_2$, two major differences in the viscoelasticity changes of the layers are observed between the two polysaccharides. First, the PGA layer exhibits a significantly larger elastic shear modulus and shear viscosity when compared to those of the alginate layer. It suggests that the PGA layer is generally more rigid with a smaller water content. Second, the two polysaccharides show diverging viscoelasticity with increasing ionic strength. At high ionic strength, PGA viscoelastic properties significantly rise, revealing the increasing rigidity of the layer, whereas alginate viscoelastic properties approach values closer to the viscoelastic properties of pure water ($\mu(H_2O) = 0$ and $\eta(H_2O) = 1.06 \times 10^{-3}$ N m^{-2} at 20 °C). This divergence in viscoelasticity between the two polysaccharides is also depicted in their coefficients of variation (Table 1). The PGA layer shows increasing coefficients of variation in the presence of calcium, whereas the alginate layer shows coefficients decreasing in magnitude. The PGA layer becomes significantly more rigid, while the alginate layer shows increasing fluidity by swelling. However, at higher ionic strength (100 mM), the two replicate alginate experiments also show some divergence. The layer of replicate 1, with its total thickness increasing at 300 mM (Figure 1b), shows a simultaneous decrease in its viscoelastic properties. Replicate 2, which reduces

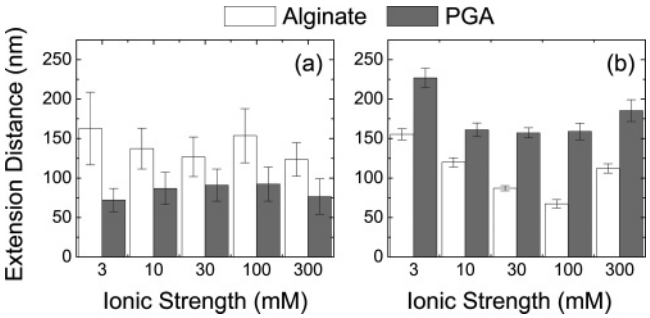

Figure 8. Variation in the pull-off distances of the adsorbed polysaccharides using AFM data as a function of ionic strength (a) in the absence and (b) in the presence of calcium. Extension distances of the adsorbed molecules or complexes are measured during the retraction and detachment of the colloidal probe from the surface after the conditioning period of the adsorbed layer at a specific ionic strength. Shown are average values with the corresponding standard errors.

its total layer thickness at high ionic strength, shows an increasing elastic shear modulus, or reducing fluidity.

3.4. Pull-Off Distances of Polysaccharide Molecules. Pull-off distance is defined as the distance characterizing the extension of the polysaccharides during the retraction of the AFM colloid probe.[39] Pull-off distances are measured by the maximal distance between the colloid probe and the substrate surface following the conditioning of the layer at a specific ionic strength. These measurements reflect the ability of the adsorbed molecules to extend away from the surface. The pull-off distance is indicative of the stretchable length of the polysaccharides or the polysaccharide complexes.

Figure 8 shows the variation of the pull-off distances as a function of the ionic composition of the solution for both polysaccharides. Because of the inherent heterogeneity in the adhesion force profiles, averages of the pull-off distances along with the corresponding standard errors are presented. In the absence of calcium (Figure 8a), the pull-off distances for both polysaccharides are quite variable as indicated by the large standard errors, with no clear dependence on ionic strength. The difference in the pull-off distance between alginates and PGAs may suggest that alginate polymers are longer or more elastic than the PGA polymers. Pull-off distances for adsorbed PGA in the presence of calcium (Figure 8b) are constant over most of the ionic strength range and indicate a stable film conformation under increasing ionic strengths. This insensitivity to increasing salt concentration was also observed for other features of the PGA layer (e.g., thickness and viscoelastic properties) as discussed earlier in this paper.

The results in Figure 8 also indicate that in the presence of calcium, PGA complexes stretch to longer distances compared to alginate complexes. A close inspection of the force profiles, such as the representative curves shown earlier in Figure 3b, clearly shows the highest number of rupture events for PGA as the AFM probe is retracted from the surface. Rupture events like those shown for PGA in Figure 3b were not observed as frequently for the alginate layers. The multiple rupture events for the PGA layer suggest the presence of several adhesion points between the PGA molecules and between the PGA molecules and the AFM particle probe. The alginate pull-off distances in the presence of calcium (Figure 8b) appear to be similar or shorter (at high ionic strength) than the pull-off distances measured in the absence of calcium. This variation of the pull-off distances for alginate indicates that the increase in ionic strength reduces electrostatic repulsion and allows the formation of intramolecular bridging with calcium. Such complexation, in turn, results in the reduction of the stretching length or elasticity of the alginate. The alginate complexes also were shown to break free from the AFM probe in a single rupture event (Figure 3b). Such behavior confirms the divergent changes in structure adopted by the two polysaccharide gel layers in the presence of calcium.

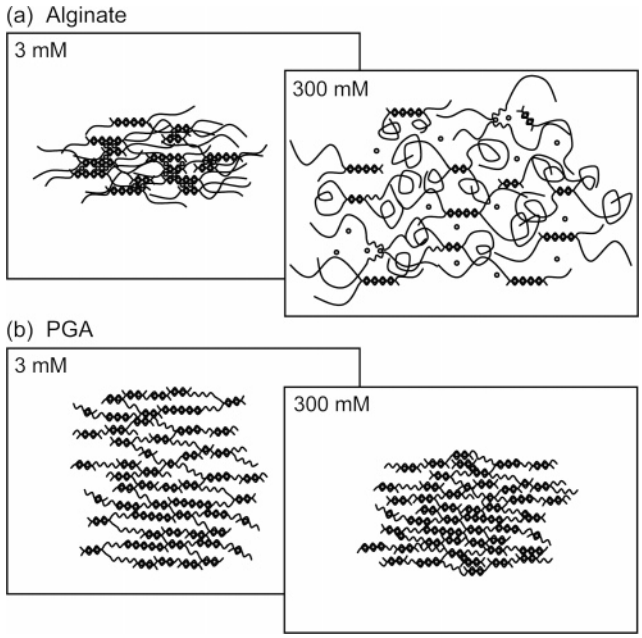

Figure 9. Mechanistic interpretation of the structural changes occurring in (a) the alginate and (b) the PGA gel matrix cross-linked with calcium ions as the ionic strength of the solution increases. Each scheme represents the state of the gel layer at a specific ionic condition in the presence of calcium. The gray dots represent calcium ions, and the lines represent the polysaccharides.

3.5. Mechanistic Interpretation of the Divergence in Polysaccharide Adsorption in the Presence of Calcium. Both the QCM-D and the AFM experiments demonstrated the strong influence of calcium on polysaccharide complexation during adsorption at the solid interface. The presence of calcium in solution induces the formation of strong bridges between polysaccharide macromolecules[8,12−14] that control the adsorption phenomena. Such specific interactions dominate the other interaction forces, such as van der Waals interaction and hydrogen bonding, that were governing the polysaccharide adsorption in the absence of calcium.[21] At low ionic strength, both polysaccharides formed a thick and fluid gel layer through divalent cation sequestration. However, the changes in the layer structures observed in response to ionic strength increases revealed differences in the complexation mechanism between the two studied polysaccharides. Assuming that the previously introduced model of the egg-box structure is the main mechanism responsible for causing these two polysaccharides to form gels in the presence of calcium,[15] we can base our discussion on the different abilities of galacturonic and guluronic acids to sequester calcium and on the respective abundance of these two monomers in PGA and alginate molecules. An illustrated mechanistic interpretation of our results is provided in Figure 9.

The divergence in the structural properties of the two polysaccharide layers can be explained as a response to their efficiency to complex calcium and the resulting complexes to form cohesive gel structures. It was shown that calcium-induced gelation follows a two-step process—first the initial dimerization of the polysaccharide molecules, followed by dimer−dimer aggregation.[40,41] The first step induces the formation of strong

and specific associations between guluronates or galacturonates and the divalent cations, whereas the second is mainly governed by electrostatic interactions with no specificity. Alginates, with a lower abundance of guluronic sequences, strongly depend on the formation of dimer−dimer associations for a cohesive gel formation. However, this aggregation can be easily disrupted by competing ions. The ion-exchange process, which has been extensively described in the literature,[31,33,42−44] as well as the change in conformation of the polysaccharides[39,45] are likely to be responsible for the observed swelling of the gel matrix (Figure 9a).[46] This swelling pressure induced by the penetration of water and salts into the adsorbed layer could cause dissociation of the dimer−dimer aggregation. The subsequent stretching of the cross-linked guluronate regions creates a weakened gel structure and could consequently fragment the matrix. The limited extension of the alginate matrix during pull-off in the presence of calcium when compared to PGA is the result of the weaker association of the polysaccharides by dimer aggregation.

The galacturonate system was shown to exhibit a more efficient dimerization conformation.[47] This system allows formation of numerous van der Waals contacts, sequestration of more calcium ions per sugar monomer compared to the guluronate system, and formation of a rich intermolecular hydrogen-bonding network. This higher efficiency suggests that the minimal critical length of galacturonate chains to form a stable junction is shorter than that of guluronic residues (Figure 9b). Therefore, PGA is better able to form a stable gel matrix almost uniquely based on dimerization of short galacturonate sequences from a large number of polysaccharides. The larger pull-off distance and the numerous rupture events observed for PGA complexes confirm the formation of abundant strong associations in the polymer matrix. This type of complexation between the polysaccharides allows the matrix to stretch further by gradual fragmentation of the calcium bridges until the polymers break free from the AFM probe. The formed dimer network is rigid and dense, making the PGA gel matrix impermeable to potassium ions. It is likely that the accumulation of monovalent salts outside the gel structure induces an osmotic flow of water outside the layer. This reduction in water content causes a decrease in the fluidity of the film and a subsequent decrease in its thickness.

4. Conclusion

QCM-D and AFM experiments were shown to be complementary in studying polysaccharide adsorption on a solid substrate under flow conditions. PGAs and alginates, two polysaccharides known for their ability to efficiently sequester calcium ions to form gel-like structures, exhibited significant differences in the properties of the gel matrices formed in the presence of divalent calcium ions. The difference in viscoelasticity of the adsorbed film and the magnitude of the interaction forces measured allowed a better understanding of the role of the polysaccharide chemical composition and structure in relation to the sensitivity of the complexed matrix to increasing ionic strength. Our findings demonstrate that a polysaccharide matrix complexed with calcium ions can adopt divergent swelling behaviors as the conditions of the surrounding solution change. The efficiency of the specific acidic monomers to complex the divalent cations and their abundance in polysaccharide molecules play a crucial role in the definition of the sensitivity of the gel structure to resist high salt concentration environments.

Acknowledgment. Funding was provided by the National Science Foundation (NSF) (Grant No. BES 0228911) and by the NSF Science and Technology Center for Advanced Materials for Purification of Water with Systems. We thank Dr. Paul Van Tassel for use of the QCM-D.

References and Notes

(1) Rompp, W.; Beitlich, R. *Am. Dyest. Rep.* **1983**, *72* (2), 31−32.
(2) Brownlee, I. A.; Allen, A.; Pearson, J. P.; Dettmar, P. W.; Havler, M. E.; Atherton, M. R.; Onsoyen, E. *Crit. Rev. Food Sci. Nutr.* **2005**, *45* (6), 497−510.
(3) Uludag, H.; De Vos, P.; Tresco, P. A. *Adv. Drug Delivery Rev.* **2000**, *42* (1−2), 29−64.
(4) Reis, C. P.; Neufeld, R. J.; Vilela, S.; Ribeiro, A. J.; Veiga, F. *J. Microencapsulation* **2006**, *23* (3), 245−257.
(5) Srivastava, R.; Brown, J. Q.; Zhu, H. G.; McShane, M. J. *Macromol. Biosci.* **2005**, *5* (8), 717−727.
(6) Kekkonen, J.; Lattu, H.; Stenius, R. *J. Pulp Pap. Sci.* **2002**, *28* (1), 6−12.
(7) Elbert, D. L.; Hubbell, J. A. *Abstr. Pap. Am. Chem. Soc.* **2000**, *219*, U583−U583.
(8) Ravanat, G.; Rinaudo, M. *Biopolymers* **1980**, *19* (12), 2209−2222.
(9) Thakur, B. R.; Singh, R. K.; Handa, A. K. *Crit. Rev. Food Sci. Nutr.* **1997**, *37* (1), 47−73.
(10) Draget, K. I.; Smidsrod, O.; Skjakbraek, G., Alginates from Algae. In *Polysaccharides and Polyamides in the Food Industry: Properties, Productions, and Patents*; Steinbüchel, A., Rhee, S. K., Eds.; John Wiley & Sons: Weinheim, Germany, 2005.
(11) Smidsrod, O. *Carbohydr. Res.* **1970**, *13* (3), 359−372.
(12) Morris, E. R.; Rees, D. A.; Thom, D.; Boyd, J. *Carbohydr. Res.* **1978**, *66* (1), 145−154.
(13) Thom, D.; Grant, G. T.; Morris, E. R.; Rees, D. A. *Carbohydr. Res.* **1982**, *100* (1), 29−42.
(14) Davis, T. A.; Llanes, F.; Volesky, B.; Mucci, A. *Environ. Sci. Technol.* **2003**, *37* (2), 261−267.
(15) Grant, G. T.; Morris, E. R.; Rees, D. A.; Smith, P. J. C.; Thom, D. *FEBS Lett.* **1973**, *32* (1), 195−198.
(16) Siew, C. K.; Williams, P. A.; Young, N. W. G. *Biomacromolecules* **2005**, *6* (2), 963−969.
(17) Decho, A. W. *Carbohydr. Res.* **1999**, *315* (3−4), 330−333.
(18) Sartori, C.; Finch, D. S.; Ralph, B.; Gilding, K. *Polymer* **1997**, *38* (1), 43−51.
(19) Potter, K.; Balcom, B. J.; Carpenter, T. A.; Hall, L. D. *Carbohydr. Res.* **1994**, *257* (1), 117−126.
(20) Ouwerx, C.; Velings, N.; Mestdagh, M. M.; Axelos, M. A. V. *Polym. Gels Networks* **1998**, *6* (5), 393−408.
(21) de Kerchove, A. J.; Elimelech, M. *Macromolecules* **2006**, *39* (19), 6558−6564.
(22) Frank, B. P.; Belfort, G. *Langmuir* **1997**, *13* (23), 6234−6240.
(23) Marx, K. A. *Biomacromolecules* **2003**, *4* (5), 1099−1120.
(24) Butt, H. J.; Cappella, B.; Kappl, M. *Surf. Sci. Rep.* **2005**, *59* (1−6), 1−152.
(25) Rodahl, M.; Hook, F.; Krozer, A.; Brzezinski, P.; Kasemo, B. *Rev. Sci. Instrum.* **1995**, *66* (7), 3924−3930.
(26) Iruthayaraj, J.; Poptoshev, E.; Vareikis, A. V.; Makuska, R.; van der Wal, A.; Claesson, P. M. *Macromolecules* **2005**, *38* (14), 6152−6160.
(27) Gurdak, E.; Dupont-Gillain, C. C.; Booth, J.; Roberts, C.; Rouxhet, P. G. *Langmuir* **2005**, *21*, 10684−10692.
(28) Richter, R. P.; Brisson, A. *Langmuir* **2004**, *20* (11), 4609−4613.
(29) Notley, S. M.; Eriksson, M.; Wagberg, L. *J. Colloid Interface Sci.* **2005**, *292* (1), 29−37.
(30) Kikkawa, Y.; Yamashita, K.; Hiraishi, T.; Kanesato, M.; Doi, Y. *Biomacromolecules* **2005**, *6* (4), 2084−2090.
(31) Qin, Y. M. *Text. Res. J.* **2005**, *75* (2), 165−168.
(32) Farhat, T. R.; Schlenoff, J. B. *Langmuir* **2001**, *17* (4), 1184−1192.
(33) Crist, D. R.; Crist, R. H.; Martin, J. R.; Watson, J. R. *FEMS Microbiol. Rev.* **1994**, *14* (4), 309−313.
(34) Voinova, M. V.; Rodahl, M.; Jonson, M.; Kasemo, B. *Phys. Scr.* **1999**, *59* (5), 391−396.
(35) Vogt, B. D.; Lin, E. K.; Wu, W. L.; White, C. C. *J. Phys. Chem. B* **2004**, *108* (34), 12685−12690.
(36) Ducker, W. A.; Senden, T. J.; Pashley, R. M. *Langmuir* **1992**, *8* (7), 1831−1836.
(37) Ryden, P.; MacDougall, A. J.; Tibbits, C. W.; Ring, S. G. *Biopolymers* **2000**, *54* (6), 398−405.

(38) Lee, S.; Elimelech, M. *Environ. Sci. Technol.* **2006**, *40* (3), 980−987.
(39) Abu-Lail, N. I.; Camesano, T. A. *J. Microsc. (Oxford)* **2003**, *212*, 217−238.
(40) Seale, R.; Morris, E. R.; Rees, D. A. *Carbohydr. Res.* **1982**, *110* (1), 101−112.
(41) Morris, E. R.; Rees, D. A.; Young, G. *Carbohydr. Res.* **1982**, *108* (2), 181−195.
(42) Draget, K. I.; Steinsvag, K.; Onsoyen, E.; Smidsrod, O. *Carbohydr. Polym.* **1998**, *35* (1−2), 1−6.
(43) Qin, Y. M. *J. Appl. Polym. Sci.* **2004**, *91* (3), 1641−1645.
(44) Smidsrod, O.; Haug, A. *Acta Chem. Scand.* **1965**, *19*, 329−340.
(45) Abu-Lail, N. I.; Camesano, T. A. *Biomacromolecules* **2003**, *4*, (4), 1000−1012.
(46) Moe, S. T.; Skjakbraek, G.; Elgsaeter, A.; Smidsrod, O. *Macromolecules* **1993**, *26*, (14), 3589−3597.
(47) Braccini, I.; Perez, S. *Biomacromolecules* **2001**, *2* (4), 1089−1096.

BM060670I